American Journal of Nanosciences
2017; 3(1): 1-8
http://www.sciencepublishinggroup.com/j/ajn
doi: 10.11648/j.ajn.20170301.11

Improving the CO Sensing Properties of Ferrocene Modified Polypyrrole/Silicon Carbide Nanocomposite Films Synthesized by Electrochemical Deposition

Hamida MB Darwish[1, *], Salih Okur[2]

[1]Department of Physics, Faculty of Sciences, King Abdul-Aziz University, Jeddah, Kingdom of Saudi Arabia

[2]Department of Material Science and Engineering, Faculty of Engineering, Izmir Katip Celebi University, Izmir, Turkey

Email address:
hdarwish@kau.edu.sa (H. MB Darwish)

To cite this article:
Hamida MB Darwish, Salih Okur. Improving the CO Sensing Properties of Ferrocene Modified Polypyrrole/Silicon Carbide Nanocomposite Films Synthesized by Electrochemical Deposition. *American Journal of Nanosciences.* Vol. 3, No. 1, 2017, pp. 1-8.
doi: 10.11648/j.ajn.20170301.11

Received: December 2, 2016; **Accepted**: December 12, 2016; **Published**: March 22, 2017

Abstract: In this study, SiC nanoparticles 40 nm in diameter were added to ferrocene-modified conducting polymer (Fc-PPy) films to improve the signal/noise ratio of a sensor. The increased porosity of the Fc-PPy/SiC nanocomposite film produces a larger active surface area with more active sites available for adsorption. Electrochemical deposition was used to fabricate nanocomposite films (PPy, Fc-PPy, PPy/SiC and Fc-PPy/SiC), on both QCM and interdigitated electrodes, to measure CO concentration. All nanocomposites were characterized using XRD, SEM and TEM. The grain sizes of the nanocomposites were measured to be between 100 nm and 500 nm after electrochemical polymerization coating. IDE chemiresistor sensors and QCM piezoelectric sensors were used to investigate the potential sensing mechanisms and adsorption-desorption kinetics of Fc-PPy/SiC nanocomposite films and to compare these films with bare PPy films. The sensitivity of Fc-PPy/SiC nanocomposite sensors to CO gas was significantly improved by the effects of the chemical activation of SiC catalyst nanoparticle additives and ferrocene modified conducting polymers.

Keywords: Ferrocene Modified Polypyrrole, SiC, QCM, IDE, CO Adsorption

1. Introduction

Carbon monoxide (CO), a toxic gas, is a by-product of the combustion of organic compounds in vehicle exhaust, gas turbines and nearly every synthetic industry involved in energy production. Monitoring CO levels with highly sensitive sensors is particularly important for measuring environmental quality. Electrochemical sensors composed of conducting polymers have many advantages, including low cost, ease of fabrication, tunable selectivity and flexible processing at room temperature [1-3]. Polypyrrole (PPy) is frequently used for sensor applications due to its broad π–electron conjugated conductivity and the alternating single and double bonds in its molecular structure [4-6].

The electrical conductivity of PPy sensors is affected by the inclusion of metallic and semiconducting nanoparticles [5, 7]. Nanowires, nanomaterials, and nanotubes composed of Si, MgO, In_2O_3, and ZnO, among other compounds, have been used to develop highly sensitive semiconducting gas sensors [8, 9]. The CO detection of Pd doped PPy sensors has been found to be highly sensitive, reversible and reproducible [10].

Casals [11] showed that SiC-based MIS capacitor sensors can detect as little as 2 ppm of CO, and their abilities are minimally affected by the presence of high concentrations of CO_2 in pure nitrogen. Recently, Pallavi et al. experimentally demonstrated that PPy/SiC polymer nanocomposites (PNC) have higher conductivity than pure PPy [12]. Electron transport in PNCs is related to the variable range hopping conduction mechanism that results from a temperature-dependent conduction process. Polypyrrole conducting polymers functionalized with iron and its complexes [5, 7] have been found to be very sensitive and selective to CO gas due to their catalytic properties. In our previous study, the effect of ferrocene functionalization on polypyrrole thin films was investigated by analyzing the adsorption and desorption kinetics of a carbon monoxide gas for sensor applications using a quartz microbalance technique [8].

The QCM results showed that ferrocene-functionalized polypyrrole Fc-PPy coated QCM is highly sensitive to CO gas compared to bare PPy sensors. Silicon carbide (SiC) was used in this study due to its tunable wide band gap structure, which is suitable for high-temperature chemical resistance, and its hardness [12, 13]. In this study, SiC nanoparticles 40 nm in diameter were added to ferrocene-modified conducting polymers (Fc-PPy). QCM was used to investigate the potential sensing mechanisms and adsorption-desorption kinetics of Fc-PPy/SiC films compared with bare PPy thin films. Electrochemical deposition was used to fabricate nanocomposite films (PPy, Fc-PPy, PPy/SiC and Fc-PPy/SiC) on both QCM and IDE interdigitated electrodes (IDE) to measure CO concentration. The sensitivity of these sensors to CO gas improved significantly as a result of the effects of chemical activation of SiC catalyst nanoparticle additives and ferrocene modified conducting polymers.

2. Experimental Details

2.1. Materials

Chemical materials were obtained from Aldrich Chemical Co. All chemicals were of analytical grade and were used without further purification. High purity SiC nanoparticles (> 99.9%) with an average particle size of 40 nm, a specific surface area of 39.8 m^2/g, and a bulk density of 0.11 g/cm^3 were obtained from Beijing Deke Daojin Science and Technology Co. (China). To electrochemically fabricate PPy nanocomposite thin films, SiC nanoparticles were added during the synthesis of polypyrrole monomers.

2.2. Preparation of Polypyrrole and Fc-PPy/SiC Nanocomposite Films

Ferrocene modified and unmodified polypyrrole nanocomposites were prepared by the electrochemical oxidative polymerization of pyrrole and ferrocene-pyrrole monomers with and without SiC nanoparticles. 1-(2-carboxyethyl) pyrrole was obtained through the hydrolysis of 1-(2-cyanoethyl) pyrrole (Py-CN) using a previously published method [14]. Electrochemical polymerization was performed in a solution of Fc-PPy monomer (0.1 *m*m) and 1.0 M p-toluene sulfonic acid sodium salt at a fixed voltage of 1.2 V vs. Ag/AgCl. Then, the Fc-PPy polymer was electrochemically synthesized on Au working electrodes at an injected charge density of 100 *m* C/cm^2 in the form of a thin film.

Analytical grade ammonium persulphate (APS) was used as an oxidizing agent. Chemical polymerization was performed in a beaker by mixing 0.1 M aqueous solution of pyrrole and 0.1 M of APS in a 1:1 ratio by volume. Three cycles of electrochemical polymerization were performed with a 50 mV scanning speed between 0 V-1.2 V with current between 100 µA and 4 mA, as shown in Figure 1. Each solution was separately prepared by chemical reduction, and 1 mg of SiC nanoparticles was added. To the SiC dispersed solution, 32 µL of PPy polymer monomer, 4 mL of media, and 16 µL of ferrocene were added for electropolymerization. Both PPy and SiC nanoparticles were deposited simultaneously using electrochemical deposition to form a stable PPy/SiC nanocomposite thin film on gold QCM and IDE electrodes. Further details can be found in the literature [15].

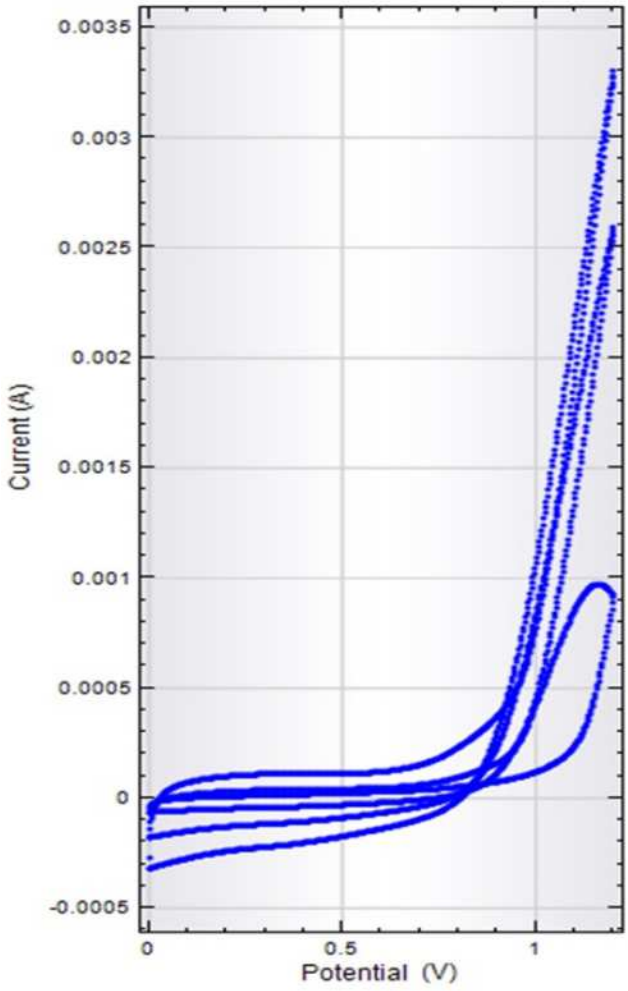

Figure 1. *Electrochemical polymerization I-V curve obtained with a 50 mV scan speed between 0 V-1.2 V and current between 100 µA-4 mA.*

2.3. QCM and IDE Measurements

Interdigitated electrodes (IDEs) with 12 fingers and 3 µm spacing were fabricated by UV photolithography, as shown in Figure 2. IDEs were used to measure electrical signals resulting from changes in the resistance of Fc-PPy/SiC nanocomposite thin films (of areas equal to $1.96\times10^{-5} m^2 \cong 0.2\mu m^2$) using a source meter (Keithly 2636A USA), while QCM was used to measure changes in frequency due to mass uptake during the adsorption and desorption of CO molecules. Both QCM and IDE data were acquired simultaneously from samples mounted in a gas measurement chamber. The same experimental setup with a 2-channel gas sensor test system was used as before more details will be found in ref. [15 & 16].

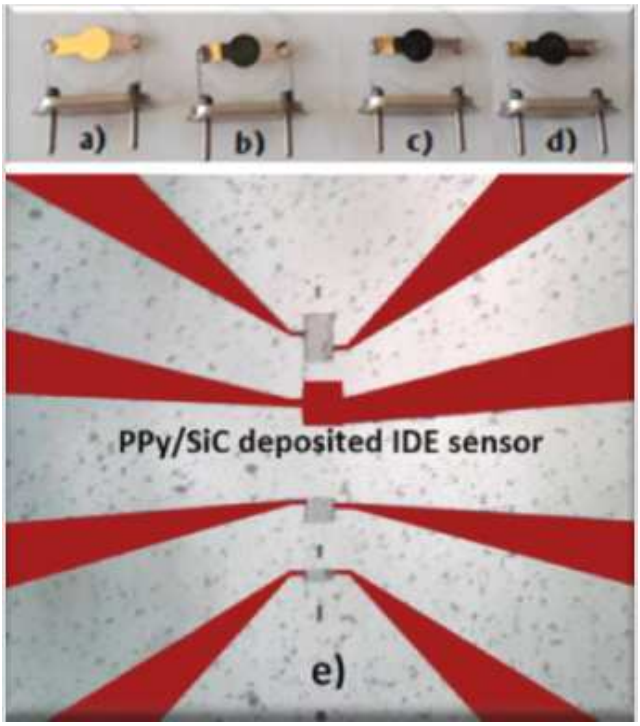

Figure 2. *Fabrication of PPy/SiC nanocomposite thin films deposited simultaneously on both gold QCM and gold IDE electrodes with 3 μm spacing: empty (a), PPy (b), PPy-Fc (c), PPy/SiC deposited QCM electrodes (d), PPy/SiC deposited IDE electrodes (e).*

The crystal structures of the Fc-PPy/SiC nanocomposites were characterized by X-ray diffraction (XRD). Powder XRD analysis of the samples was performed with a Bruker D2 PHASER X-ray diffraction tool that enabled the analysis of poly-crystalline material using DIFFRAC SUITE software with a LYNXEYE detector diffraction system operating with a Cu K_α radiation source (λ =1.5406 Å). The incident ω angle was 5° and XRD scans were recorded from 7° to 77° for 2θ with a 0.050° step width and each step lasting 60 s. Fourier Transform Infrared Spectroscopy (FT-IR) with Perkin Elmer Model absorption spectra were measured over a range of wavelengths from 2500 to 600 cm^{-1} at 25°C to determine the chemical structures of nanocomposite films produced at room temperature for 30 min in air using an electrochemical process. The surface morphologies and elemental analyses of the nanocomposite films were conducted using SEM (JEOL JSM 6060). Transmission electron microscope (TEM) images were taken with JEOL JEM-2100F.

3. Results and Discussion

3.1. Phase Analysis

XRD patterns of PPy nanocomposite samples are given in Figure 3 for PPy, Fc-PPy, PPy/SiC, Fc-PPy/SiC and SiC samples. In the XRD results, broad peaks at 2θ=18° and 2θ=28° show the semicrystalline structures of the formed polypyrrole and polypyrrole/SiC nanocomposites.

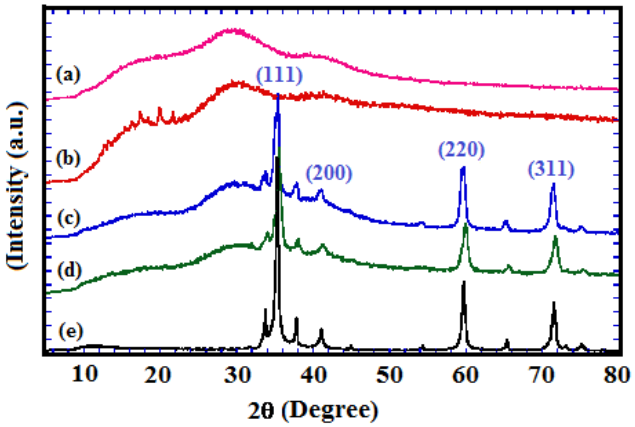

Figure 3. *XRD patterns of (a) PPy, (b) Fc-PPy, (c) PPy/SiC, (d) Fc-PPy/Si and (e) SiC samples.*

Table 1. *XRD analysis.*

2θ	θ	d (for n=1)	hkl
35.33°	17.7°	2.53	111
37.6°	18.8°	2.4	200
41.2°	20.6°	2.18	020
59.7°	29.85°	1.54	220
65.2°	32.6°	1.43	300
71.2°	35.6°	1.32	311

The d spacing between the crystal planes was calculated using Bragg's equation, ($n\lambda = 2d\sin\theta$), where n is an integer, λ is the wavelength of the Cu K_α radiation source, and θ is the angle between the incident ray and the crystal planes. The XRD analysis results are shown in Table 1. The d spacing for the four major peaks at 2θ = 35.330, 37.6, 59. 7, and 71.2 was calculated as 2.53, 2.4, 1.54 and 1.32 Å corresponding to the (111), (200), (220), and (311) planes of SiC crystals, which is consistent with the standard XRD file PDF No. 29-1129. The major SiC peaks shifted toward a lower diffraction angle than those of pure SiC nanoparticles, indicating the formation of nanocomposites. This is consistent with SEM and TEM results, as will be explained.

3.2. FT-IR Analysis

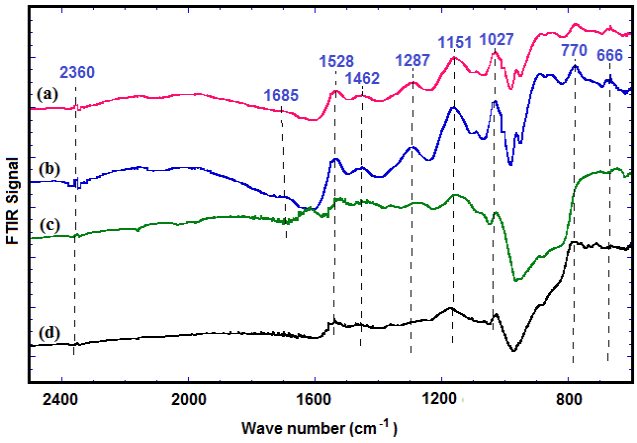

Figure 4. *FT-IR spectra of (a) PPy, (b) Fc-PPy, (c) PPy/Si, and (d) Fc-PPy/SiC samples.*

FT-IR spectra of polypyrrole nanocomposite films

prepared by electrochemical deposition are given in Figure 4 for PPy, Fc-PPy, PPy/SiC, and Fc-PPy/SiC nanocomposite samples. The characteristic peaks at 1528 cm^{-1} and 1462 cm^{-1} correspond to the fundamental vibrations of the polypyrrole ring. The band at 1287 cm^{-1} corresponds to C-H deformation. Other low intensity peaks are observed at approximately 2927 cm^{-1}-2814 cm^{-1} and can be attributed to aromatic C-H stretching vibrations. The peaks at 1685 m^{-1} and 770 cm^{-1} represent C=N and C-N bonds. The C-H bond in-plane deformation vibration is seen at 985 cm^{-1}, and the C-C out-of-plane ring deformation vibrations or C-H rocking are seen at 666 cm^{-1}.

3.3. SEM Analysis

SEM images of pure PPy and Fc-PPy/SiC nanocomposite structures were obtained at 10 kV with an image acquisition time of 30 μs at a magnification of 80,000x. Figure 5 shows SEM images of the nanocomposite structures SiC, pure polypyrrole (PPy), polypyrrrole (PPy/SiC), ferrocene-polypyrrole (Fc-PPy), and Fc-PPy/SiC with different nonograin sizes. In Figure 5.a, the SEM image of SiC nanoparticles shows a typical particulate nanostructure with a uniform size distribution. Figure (5. b) shows an SEM image of pure PPy, while Figure 5.c reveals an SEM image with large grain sizes as a result of a 50% Fc-50%PPy conjugation. Figure 5.d corresponds to PPy-SiC with a ratio of 25% to 75%. The observed bright spots on the SiC nanoparticles are due to contrast arising from the collected electrons. Figure 5.e shows an SEM image of a sample composed of 25% PPy-Fc and 75% SiC. The reaction between the nanoparticle sizes of SiC and the grain sizes of conjugated PPy-Fc, increase the binding strength of the composite and make the SiC surface covered with PPy and Fc-PPy more spherical, as shown in Figures 5.d and 5.e.

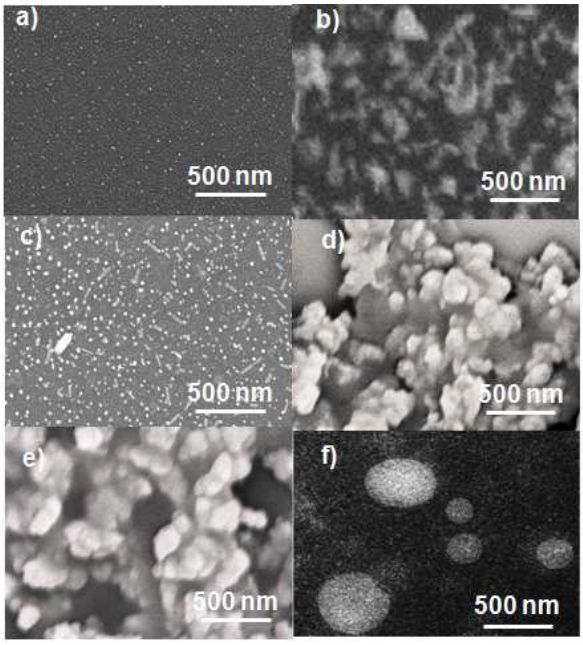

Figure 5. *SEM images of (a) SiC, (b) PPy, (c) Fc/SiC, (d) Fc-PPy, (e) PPy/SiC & (f) Fc-PPy/SiC samples.*

3.4. TEM Results

Figure 6 shows TEM images of SiC, PPy, Fc-PPy, PPy/SiC, and Fc-PPy/SiC nanocomposites. The grain sizes of the nanostructures are approximately 100 nm-500 nm. The SiC nanocomposite structures covered with polypyrrole derivatives are larger than those composed of pure SiC. Figure 6.a shows a TEM micrograph demonstrating the size of SiC nanoparticles. PPy increases the surface areas of SiC and Fc, as seen in Figures 6.c, 6.d, and 6.e. Figure 6.f shows a low magnfication TEM micrograph of Fc-PPy/SiC.

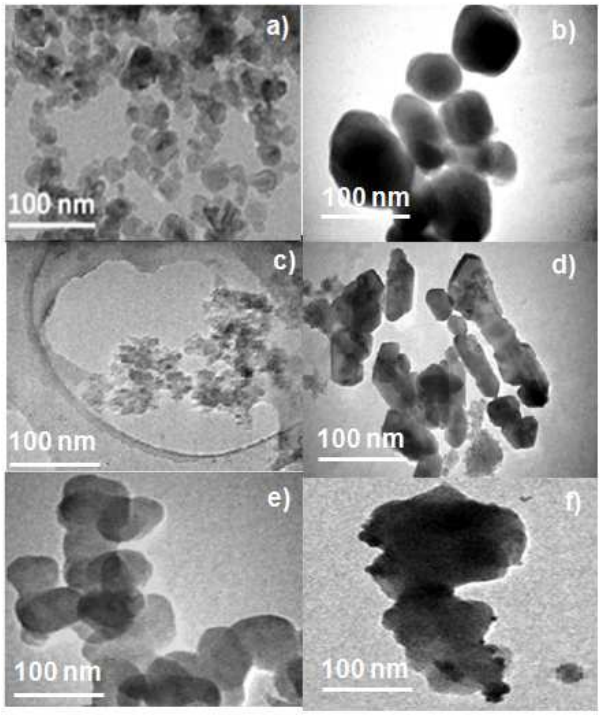

Figure 6. *TEM images of (a) SiC, (b) PPy, (c) Fc/SiC, (d) Fc-PPy, (e) Fc/SiC & (f) Fc-PPy/SiC low sample.*

3.5. QCM and IDE Results

QCM and IDE CO gas sensors have been designed with sensitive nanocomposite thin films containing ferrocene-modified conducting polymers (Fc-PPy) and SiC nanoparticles. QCM was used to investigate the potential sensing mechanisms and adsorption-desorption kinetics of SiC nanoparticles dispersed in Fc-PPy films. Nanocomposite films were fabricated using electrochemical synthesis on microfabricated interdigitated electrodes to enable the electronic readout of sensor responses to measure CO concentration. The addition of SiC nanoparticles was meant to improve the porosity of the composite film structure to increase the active surface area and obtain more available active sites for adsorption, which significantly increases the signal/noise ratio of the sensor. The time dependence of the quantity of absorbed CO molecules on the film surface, Δm_t, can be defined by the Langmuir Isotherm Model as [15].

$$\Delta m_t = \Delta m_\infty \left(1 - e^{-t/\tau_m}\right), \qquad (1)$$

similarly

$$\Delta R_t = \Delta R_\infty \left(1 - e^{-t/\tau_R}\right) \quad (2)$$

where $\tau^{-1} = k_a\ [CO\,molecules] + k_d$, Δm_∞ is the maximum adsorbed mass of CO molecules and ΔR_∞ is the maximum corresponding resistance between the IDE electrodes due to local charge depletion as a result of the interaction of CO molecules on PPy composite film surfaces over long periods of time, when t→ ∞. At higher concentrations, the Langmuir model can be used to express both QCM and IDE sensor results as follows:

$$\Delta m_t = \Delta m_\infty \times \frac{K_m \times C(t)}{1 + K_m \times C(t)} \text{ and } \Delta R_t = \Delta R_\infty \times \frac{K_R \times C(t)}{1 + K_R \times C(t)}, \quad (3)$$

where K_m is the Langmuir adsorption constant and C (t) is the variable CO concentration in the gas cell. The conductivity of PPy is proportional to the number of conduction sites, which are uniformly distributed on the polymer surface. These sites can absorb CO molecules, thereby contributing to the conductivity. All active sites (ferrocene and SiC nanoparticles) are assumed to be homogenously distributed throughout the Fc-PPy/SiC and the probability that a gas molecule adsorbs to any site on the surface is equivalent. Nevertheless, inside the film, the diffusion process is the dominant mechanism of interaction. Each active site can only adsorb one molecule [17]. Charlesworth et al. [18] investigated the relationship between mass and conductance changes in a PPy film and found that the fractional change in resistance varies linearly with fractional mass uptake when the mass change is below 5%. The diffused mass due to adsorbed CO molecules inside the film during exposure to CO is described by Fick's equation [19] for diffusion:

$$\frac{M(t)}{M(\infty)} = 1 - \left(\frac{1}{\pi^2}\right) \sum_{n=0}^{\infty} \frac{1}{(2n+1)^2} \exp\left[\frac{-2D(2n+4)^2 \pi^2}{4L^2}\right] \propto \quad (4)$$

where *M (t)* is the mass taken up by the film at time *t*, *M (∞)* is the equilibrium mass uptake by the film, *L* is the film thickness, and *D* is the diffusion coefficient. Hence, the contribution of the diffusion term to the conductivity of PPy composite films can account for porous thin films.

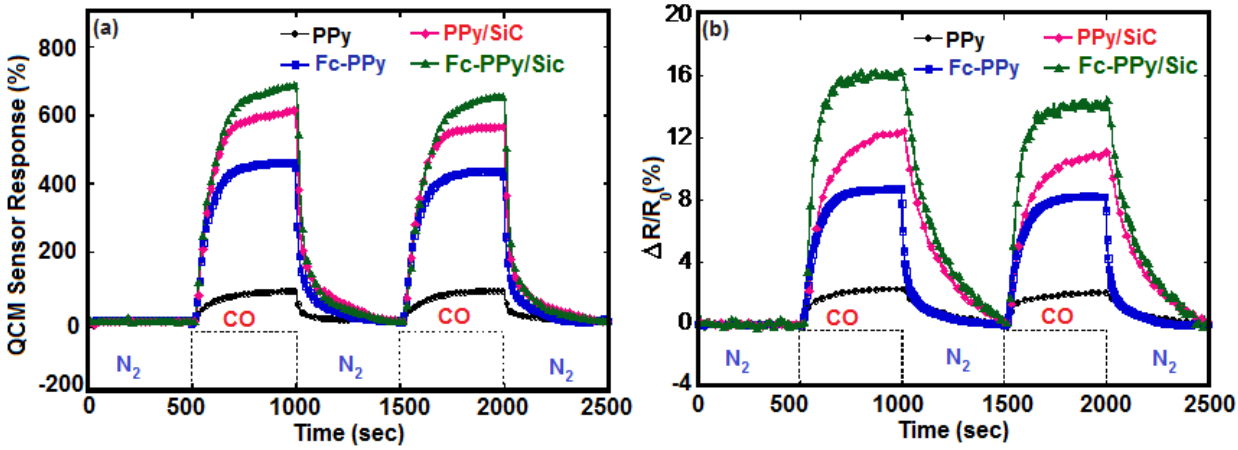

Figure 7. *Experimental sensor response: (a) QCM and (b) IDE chemiresistor responses to the interactions of CO gas molecules with pure PPy, Fc-PPy, and Fc-PPy/SiC composite thin films at room temperature.*

The experimental responses of QCM and IDE chemiresistor sensors to the interactions of CO gas molecules with pure PPy, PPy-Fc, and PPy-Fc/SiC composite thin films at room temperature are given in Figures 7.a and 7.b. The QCM frequency response is proportional to the change in mass on the QCM sensor due to adsorption and desorption according to the Sauerbrey Eq. [20]. The response times of all PPy composite thin film coated QCM sensors and IDE sensors were obtained at times corresponding to the value at the 90% maximum change in the signal, while recovery times were determined when the maximum value dropped to 10%.

Figure 8. shows the Langmuir analysis of QCM and IDE sensor responses to the interactions of CO gas molecules with pure PPy, Fc-PPy, and Fc-PPy/SiC composite thin films at room temperature: Figures 8.a and 8.b depict the nonlinear least square fit (solid lines) of the time-dependent Langmuir adsorption isotherm model applied to QCM and IDE chemiresistor sensors, respectively. Figures 8.c and 8.d show the Langmuir adsorption fit to the saturation region data at higher CO concentrations applied to the QCM and IDE chemiresistor sensors, respectively. Figures 8.e depicts the Langmuir adsorption fit to the linear region at lower CO concentrations (less than 700 ppm) applied to the QCM and IDE (Figure 8.f) chemiresistor sensors.

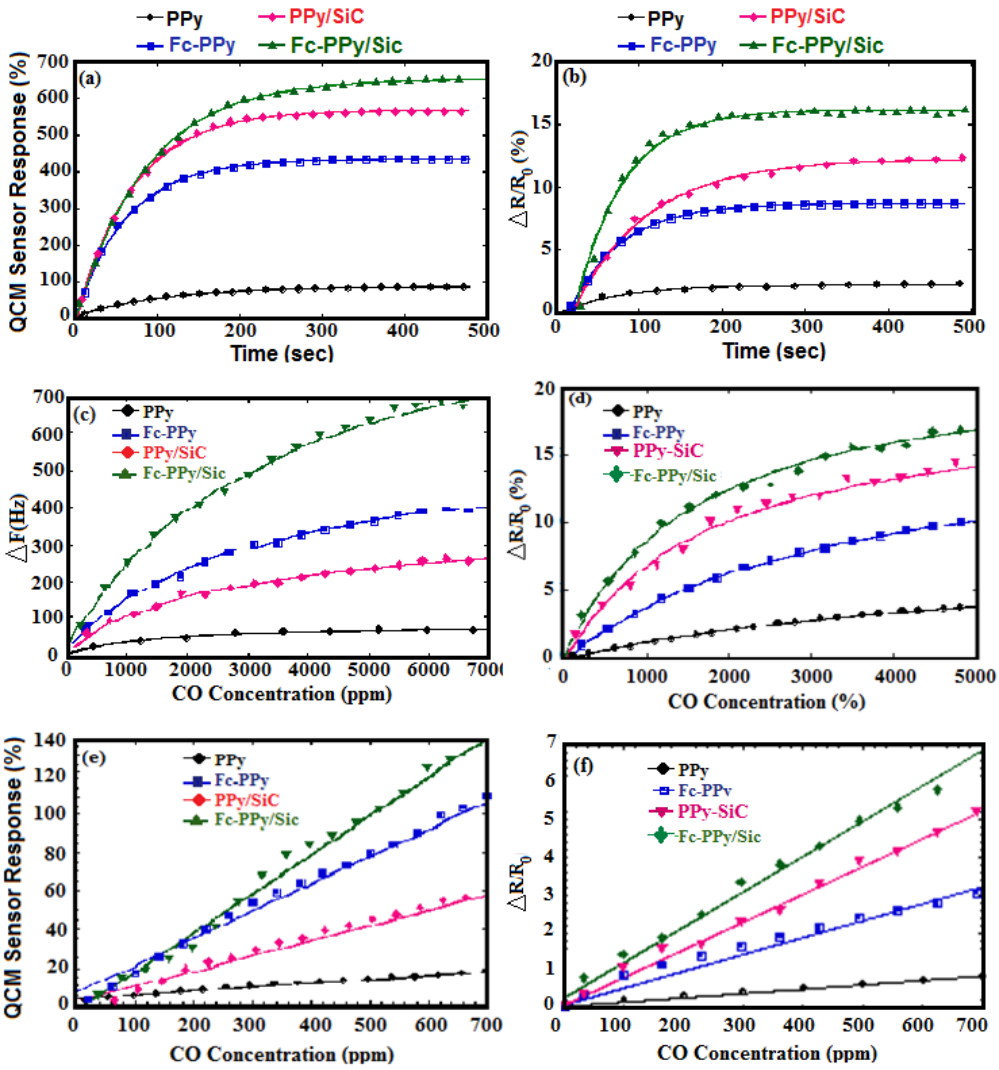

Figure 8. *Analysis of the QCM and IDE sensor responses to the interactions of CO gas molecules with pure PPy, Fc-PPy and Fc-PPy/SiC composite thin films at room temperature: (a) The time dependent Langmuir adsorption least square fit (solid lines) applied to the QCM, (b) IDE chemiresistor, (c) Langmuir adsorption fit to the saturation data at higher CO concentrations applied to the QCM, (d) IDE chemiresistor, (e) Langmuir adsorption fit to the linear region at lower CO concentrations less than 700 ppm applied to the QCM, and (f) IDE chemiresistor sensors.*

The results of characteristic sensing parameter analysis of the sensor responses of QCM and IDE chemiresistor sensors to the interactions of CO gas molecules with pure PPy, Fc-PPy, and Fc-PPy/SiC composite thin films at room temperature are given in Table 2.

Table 2. *The experimental sensor responses of QCM and IDE chemiresistor sensors to the interactions of CO gas molecules with pure PPy, Fc-PPy, PPy/SiC, and Fc-PPy/SiC composite thin films at room temperature.*

Experimental Sensor Responses	**PPy**	**Fc/PPy**	**PPy/SiC**	**Fc-PPy/SiC**
Max. QCM Sensor response (%)	89	462	622	692
Max IDE Sensor response (%)	2.3	8.8	12.4	16.4
QCM Response time (s)	260	170	180	176
QCM Recovery time (s)	110	125	180	130
IDE Response time (s)	135	170	150	140
IDE Recovery time (s)	360	130	360	360
QCM Adsorption rate K_a	16.22	28.5	34.63	38.12
QCM Desorption rate K_d	3.1E-03	5.45E-03	6.62E-03	7.29E-03
Langmuir adsorption constants were obtained by QCM data fitting	2.6326	3.1425	3.8235	6.7649
Langmuir adsorption constants were obtained by IDE chemiresistor data fitting	1.6627	2.9378	5.8174	6.4398
Linearity coefficients (% / ppm) were obtained by QCM data fitting	0.0208	0.079	0.1435	0.205
Linearity coefficients (% / ppm) were obtained by IDE chemiresistor data fit	1.6E-03	4.5E-03	7.4E-03	9.4E-03

The results show that the maximum QCM sensor response increased 5.2 times for Fc-PPy, 7.0 times for PPy/SiC, and 7.8 times for Fc-PPy/SiC composite thin films compared to pure PPy films. Maximum IDE sensor responses increased approximately 3.8 times for Fc-PPy, 5.4 times for PPy/SiC, and 7.1 times for Fc-PPy/SiC composite thin films compared to pure PPy films. A correlation between Δm_t (the mass of the adsorbed molecules) and ΔR_t (corresponding resistance between the IDE electrodes) can be obtained as $\Delta R_t = C_{\text{orm X}} \Delta m_t$, where C_{Rm} is related to the diffusion coefficient of the films depending on the porosity and thickness of the composite films. The correlation constant C_{Rm} between QCM and IDE sensor responses was obtained as 0.74 for Fc-PPy, 0.77 for PPy/SiC, and 0.92 for Fc-PPy/SiC composite thin films. This indicates that porosity increases the correlation coefficient between QCM and IDE sensors.

The response times of IDE chemiresistor sensors are shorter than those of QCM sensors. On the other hand, the recovery time required by QCM sensors is twice that of IDE chemiresistor sensors. The adsorption rate (K_a) is of Fc-PPy/Si is more than double that of bare PPy. Similar increases were found in the desorption rates obtained from the nonlinear least square fit to the time dependent Langmuir model. The Langmuir adsorption constant obtained from QCM data fitting is larger than the Langmuir adsorption constant obtained from IDE chemiresistor data fitting to the saturation data at higher CO concentrations. The linearity coefficient for QCM and IDE sensor responses at low CO concentrations (less than 100 ppm) were 0.205 (%)/ppm and 9, $4x10^{-3}$ %/ppm, respectively.

The decay in the second cycle of electrical resistance is related to the possible diffusion of CO in Fc-PPy/SiC nanocomposite films. The change in IDE electrical resistance was explained by the formation of polarities [21] due to the interaction of highly polar CO with an electron donating nitrogen atom in pyrrole. In addition, the interaction of CO with Fe complexes in the structure of the Fc-PPy composite around Fe moieties causes a change in the electrical signal due to the subsequent depletion of free charge carriers. The electrically conductive polymer provides efficient electron transfer in the conduction band as a response from the electrode surface of the gas sensor. Thus, the sensitivity and selectivity of the analyzed sensors for CO gas significantly improved due to the effects of the chemical activation of SiC catalyst nanoparticle additives and the ferrocene modified conducting polymer.

A potential charging effect due to the interaction of CO and SiC grains surrounded by conducting polymers modified with ferrocene is suggested by Figure 9. The gas sensing ability of the composite coated sensors tested was improved by the porous structure and induced functional groups of ferrocene and by the conducting polymer itself.

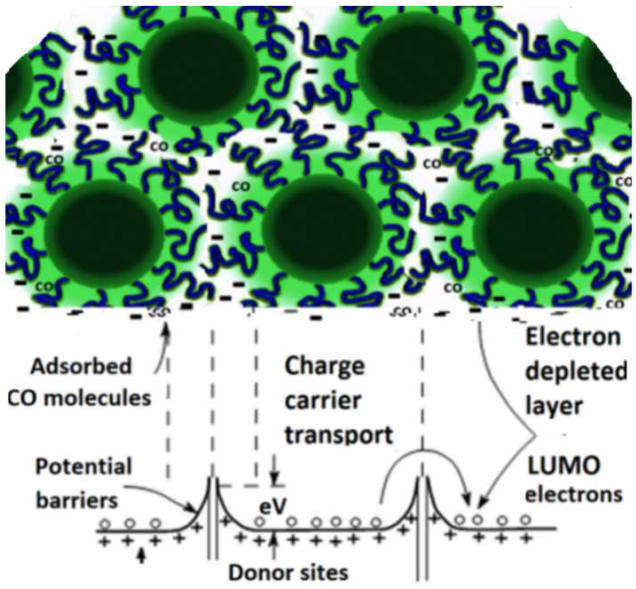

Figure 9. *Possible charging due to CO interactions with SiC grains coated with ferrocene modified conducting polymer.*

A three-step treatment was used to improve the gas sensing mechanism. First, the induced functional groups attract the target gas to the surface of the gas sensor via induced functional ferrocene groups. Second, the pore structure significantly increases the amount of adsorbed gas due to an increased number of active sites on a larger surface area. Third, the electrically conductive polymer provides an efficient transfer of conductive response from the surface of the gas sensor to the electrodes. In total, the sensitivity of the tested sensors for CO gas was significantly improved based on the effects of chemical activation, SiC nanoparticle additives, and a ferrocene modified conducting polymer.

4. Conclusions

In summary, the effect of ferrocene functionalization on polypyrrole thin films was investigated by analyzing the adsorption and desorption kinetics of carbon monoxide gas sensors using a quartz microbalance technique. Doping with SiC yields an approximately 7.8 fold increase in QCM and a 7.1 fold increase in IDE chemiresistor sensitivities compared to bare PPy thin films. SiC nanoparticles improve the porosity of the composite film structure of ferrocene conjugated polypyrrole conducting polymers. The QCM and IDE results of Fc-PPy/SiC illustrate that the frequency responses of coated QCM are highly sensitive to variations in CO gas concentration as compared to bare thin films. Using ferrocene modified PPy/SiC nanocomposite films synthesized via electrochemical deposition improves the sensitivity of CO sensor applications

Acknowledgements

This project was funded by the National Plan for Science, Technology and Innovation (MAARIFAH) King Abdulaziz

City for Science and Technology, KSA, award number (10-NAN1407-03). The authors also, acknowledge with thanks Science and Technology Unit, King Abdulaziz University, Jeddah for technical support"

References

[1] Ahmed, N.; Upadhyaya, M.; Kakati, D. K. Synthesis of nanostructured Polyaniline in dodecyl sulphuric acid (DSA) mediated Miceller medium with isopropyl alcohol as cosurfactant. *Res. J. Chem. Environ.* 2012, *16*, 19-25.

[2] Alessio, P.; Ferreira, D. M.; Job, A. E.; Aroca, R. F.; Riul,, A.; Constantino, C. J. L.; Pérez González, E. R. Fabrication, structural characterization, and applications of Langmuir and Langmuir-Blodgett films of a poly (azo)urethane. *Langmuir* 2008, *24*, 4729-4737.

[3] Alves, M. R. A.; Calado, H. D. R.; Donnici, C. L.; Matencio, T. Electrochemical polymerization and characterization of new copolymers of 3-substituted thiophenes. *Synth. Met.* 2010, *160*, 22-27.

[4] Kate, K. H.; Damkale, S. R.; Khanna, P. K.; Jain, G. H. Nano-silver mediated polymerization of pyrrole: synthesis and gas sensing properties of Polypyrrole (PPy)/Ag nano-composite. *J. Nanosci. Nanotech.* 2011, *11*, 7863-7869.

[5] Amer, W. A.; Wang, L.; Amin, A. M.; Ma, L. A.; Yu, H. J. Recent progress in the synthesis and applications of some ferrocene derivatives and ferrocene-based polymers. *J. Inorg. Organomet. Polym. Mater.* 2010, 20 605-615.

[6] Bai, H.; Shi, G. Gas sensors based on conducting polymers. *Sensors* 2007, *7*, 267-307.

[7] Paul, S.; Chavan, N. N.; Radhakrishnan, S. Polypyrrole functionalized with ferrocenyl derivative as a rapid carbon monoxide sensor. *Synth. Met.* 2009, *159*, 415-418.

[8] Zeng, W.; Liu, T.; Wang, Z. Enhanced gas sensing properties by SnO2 nanosphere functionalized TiO_2 nanobelts. *J. Mater. Chem.* 2012, *22*, 3544-3548.

[9] Dan, Y.; Evoy, S.; Johnson, A. Chemical gas sensors based on nanowires. *arXiv preprint arXiv* 2008 *0804.4828.*

[10] Ameer, Q.; Adeloju, S. B. Polypyrrole-based electronic noses for environmental and industrial analysis. *Sens. Actuators B Chem.* 2005, *106*, 541-552.

[11] Casals, O.; Romano-Rodriguez, A.; Becker, T. 1.1. 4 SiC-based MIS gas sensor for CO detection in very high water vapor environments. *Proceedings IMCS* 2012, 72-75.

[12] Mavinakuli, P.; Wei, S.; Wang, Q.; Karki, A. B.; Dhage, S.; Wang, Z.; Young, D. P.; Guo, Z. Polypyrrole/silicon carbide nanocomposites with tunable electrical conductivity. *J. Phys. Chem. C* 2010, *114*, 3874-3882.

[13] Wijesundara, M.; Azevedo, R. *Silicon Carbide Microsystems for Harsh Environments*; Springer Verlag: Berlin, 2011.

[14] Wolowacz, S. E.; Yon Hin, B. F. Y.; Lowe, C. R. Covalent electropolymerization of glucose oxidase in polypyrrole. *Anal. Chem.* 1992, *64*, 1541-1545.

[15] Darwish, H. M. B.; Okur, S. CO adsorption kinetics of ferrocene-conjugated polypyrrole using quartz microbalance technique. *Sens. Actuators B Chem.* 2014, *200*, 325-331.

[16] M. S, enel, Construction of reagentless glucose biosensor based on ferrocene.

[17] Conjugated polypyrrole, Synthetic Met., 161 (2011) 1861–1868.

[18] Li, Z.; Blum, F. D.; Bertino, M. F.; Kim, C. Understanding the response of nanostructured polyaniline gas sensors. *Sens. Actuators B Chem.* 2013, *183*, 419-427.

[19] Charlesworth, J. M.; Partridge, A. C.; Garrard, N. Mechanistic studies on the interactions between poly (pyrrole) and organic vapors. *J. Phys. Chem.* 1993, *97*, 5418-5423.

[20] Fick, A. Ueber diffusion. *Annalen der Physik.* 1855, *170*, 59–86.

[21] Kim, S. R.; Choi, S. A.; Kim, J. D.; Kim, K. J; Lee, C.; Rhee, S. B. Preparation of polythiophene LB films and their gas sensitivities by the quartz crystal microbalance. *Synth. Met.* 1995, *71*, 2027-2028.

[22] Harsányi, G. Polymer films in sensor applications: a review of present uses and future possibilities. *Sensor Rev.* 2000, *20*, 98-105.

Biography

Hamida Mohammed Bakr Darwish received her Bachelor's and Master's degrees from the Physics Department, Faculty of Sciences, King Abdulaziz University, Jeddah, KSA in 1986. She received a MPhil from the Mechanical Engineering Department of UMIST in 2001. She finished her Ph. D. in Physics in the Faculty of Science, Bristol University, UK (2006). She is currently an Assistant Professor in the Physics Depart, Sciences Faculty, KAU, Jeddah, KSA. Her current research interests are in the electrical and optical properties of nano-crystals and organic and inorganic defects in semiconductor thin films analyzed using nanotechnology techniques.